Relating Laboratory and Outdoor Exposure Of Coatings: IV. Mode and Mechanism For Hydrolytic Degradation of Acrylic-Melamine Coatings Exposed to Water Vapor In the Absence of UV Light

Tinh Nguyen, Jon Martin, and Eric Byrd—National Institute of Standards and Technology*

Acrylic-melamine coatings are known to be susceptible to hydrolysis when exposed to water or humid environments. The mode and specific pathways for hydrolytic degradation of acrylic-melamine coatings exposed to water vapor in the absence of ultraviolet light are presented. Samples of a partially methylated melamine-acrylic coating applied to CaF_2 substrates were subjected to five different relative humidity levels ranging from approximately 0 to 90% at 50°C. Coating degradation was measured with transmission Fourier transform infrared spectroscopy (FTIR) and tapping mode atomic force microscopy (AFM). In humid environments, partially methylated melamine-acrylic coatings undergo hydrolysis readily, causing considerable material loss and formation of mainly primary amines and carboxylic acids. The rate of hydrolysis increases with increasing RH. Hydrolytic degradation of acrylic-melamine coatings is an inhomogeneous process in which pits form, deepen, and enlarge with exposure. Such localized degradation mode suggests that hydrolysis of this material is an autocatalytic progression where acidic degradation products formed in the pits catalyze and accelerate the hydrolysis reactions.

INTRODUCTION

Thermoset acrylic-melamine resins are widely used for automobile exterior coatings. These materials are formed by reacting an acrylic polyol with an alkylated melamine. However, the ether crosslinks of acrylic-melamine coatings are known to be susceptible to hydrolysis when exposed to moist environments. Under outdoor and artificial acid rain environments, acrylic-melamine coatings undergo etching, which is primarily a result of acid hydrolysis of the crosslinks.[1-5] A particular attribute of etching is the localized loss of material, resulting in pitting of the coating surface. In the presence of ultraviolet (UV) light, the hydrolysis process becomes more complex. For example, the hydrolysis in Miami, FL, has been observed to be faster than that in Phoenix, AZ.[6] Numerous studies using controlled environments also showed that, in the presence of UV light, the hydrolysis rate is greater than the sum of dark hydrolysis and photolysis combined.[7-12] The enhanced degradation, which follows closely with the hydrolysis rate and relative humidity (RH) levels, not only occurs at the acrylic-melamine crosslink and in the melamine chains but also on the acrylic resin structure.[12] Enhanced degradation in UV/humidity conditions has been variously attributed to melamine excited-state chemistry,[7] oxidized products of formaldehyde,[9] catalysis by carboxylic acids produced by the photooxidation,[8] and chromophoric activity of formaldehyde molecules released from the hydrolysis reactions.[12]

The most comprehensive study of the hydrolysis of both fully and partially alkylated melamine coatings in the absence of UV light was conducted by Bauer.[13] He showed that the rate of hydrolysis depends on the type and concentration of acid curing agents, hydrolysis temperature, and type of melamine resin. During hydrolysis, the ether crosslinks are broken and the melamine-melamine linkages are formed, and coatings

Presented at the 79th Annual Meeting of the Federation of Societies for Coatings Technology, November 5-7, 2001, in Atlanta, GA.

*100 Bureau Dr., Mail Stop 8621, Gaithersburg, MD 20899

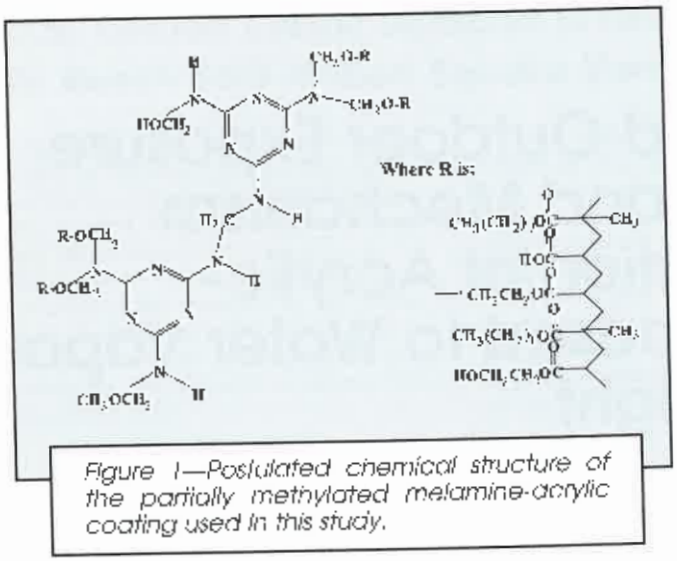

Figure 1—Postulated chemical structure of the partially methylated melamine-acrylic coating used in this study.

based on partially alkylated melamines hydrolyze much faster than do fully alkylated coatings. In mild acid conditions, the crosslinks of methylated melamine-based coatings hydrolyze faster than the unreacted methoxy groups of the melamine.[13] However, in strong acid solutions, the melamine methoxy has been reported to hydrolyze first, followed by hydrolysis of the crosslinks.[4] Hydrolysis rate dependence of melamine alkoxy ether on the chemical structure and pH is clearly revealed from solution studies by Berge and coworkers.[14,15] In mild acid solution, methylated trimethylol melamine (a partially alkylated melamine) hydrolyzes approximately 45 times faster than hexamethylol melamine (a fully alkylated melamine) while, in strong acids, the latter hydrolyzes almost 30 times faster than the former.

Despite such extensive research on the etching and hydrolysis of acrylic-melamine coatings, little information exists on the mode for the hydrolytic degradation of these materials. Further, although general hydrolysis schemes for acrylic-melamine coatings are available,[13] specific hydrolysis pathways for these materials are not known. This study presents the mode and pathways that form carboxylic acids and primary amines for the degradation of coatings based on a partially methylated melamine and a hydroxy-terminated acrylic resin exposed to water vapor in the absence of UV light. (By mode, it is meant whether the degradation is uniform across the surface or is concentrated at specific locations so as to result in pitting.) Specific hydrolysis pathways are presented based on Fourier transform infrared (FTIR) spectral evidence, and the degradation mode is proposed based on atomic force microscopy (AFM) nanoscale images of the coating microstructure and its surface morphological changes during hydrolysis. In addition, a water vapor sorption experiment was carried out to provide information on the water concentration in the film and the nature of interactions between water and acrylic-melamine coatings at different RH levels. Information on the mode and mechanism of the hydrolytic degradation is essential for understanding the controlling factors responsible for coating failures during service and for helping to develop more durable coatings. This research is part of a larger effort at the National Institute of Standards and Technology to develop metrologies for relating outdoor exposure performance with accelerated testing results and to develop improved methodologies for predicting the service lives of polymeric coatings.

EXPERIMENTAL CONDITIONS AND PROCEDURES*

Materials

Materials and sample preparations procedures were mentioned previously.[11] Briefly, samples were prepared from a mixture of a hydroxy-terminated acrylic resin and a partially methylated melamine resin. The acrylic material contained 68% normal butylmethacrylate, 30% hydroxy-ethylacrylate, and 2% acrylic acid (all are expressed in mass fraction), and the melamine resin was Cymel 325 (Cytec Industries). The ratio of acrylic resin to melamine resin was 70:30. It should be noted that, other than the 2% organic acrylic acid, no strong acid catalyst was added to this model coating formulation. Calcium fluoride (CaF_2) plates with a diameter of 100 mm and a thickness of 2 mm were used as the substrate for the exposure study due to their transparency in the 0.13 to 11.5 μm optical region and their resistance to moisture and heat.[16] Coatings were applied to CaF_2 plates by spin casting. Acrylic and melamine resins in respective solvents were mixed at the required ratio, degassed, flooded onto the substrates, and spun at 2000 rpm for 30 sec. Coated samples were then cured at 130°C for 20 min. All samples were fully cured, as evidenced by the lack of further reactions after prolonged heating at the same temperature. The cured film had a thickness of 10 μm ± 1.2 μm (the number after the ± sign indicates one standard deviation) and a glass transition temperature (T_g) of 45°C ± 2°C (by differential scanning calorimetry). *Figure* 1 shows the postulated chemical structure of the cured acrylic-melamine films used in this study.

Instrumentation and Exposure Conditions

Complete details on the exposure cell, instrumentation, and controlled systems are given in reference 17. This section briefly describes the instruments and experimental procedures pertinent to this study; that is, hydrolysis at different relative humidities in the absence of UV light.

The exposure cells were designed to simultaneously expose different sections of the same film to different conditions of RH, UV, and temperature (T). Nominal RH levels of << 1, 20, 40, 70, and 90% and at a temperature of 50°C were employed for this study. *Figure* 2a displays a photograph of three exposure cells along with the tubing system for carrying air at the desired RH and temperature, and *Figure* 2b schematically shows the

*Certain commercial products or equipment are described in this paper in order to specify adequately the experimental procedure. In no case does such identification imply recommendation or endorsement by the National Institute of Standards and Technology, nor does it imply that it is necessarily the best available for the purpose.

cross-section of the exposure cell. Each cell consisted of a 12-window aluminum frame, a quartz plate, and a 100-mm diameter CaF_2 plate with a film of the coating applied to it. One window was completely covered with an aluminum plate to prevent radiation from impinging upon the coating (designated as no-UV or covered), one exposed to full UV spectrum, and 10 contained interference filters transmitting different spectral ranges and intensities of UV light. Care was taken to ensure that no radiation strayed onto the no-UV (covered) coating area. The space between the quartz plate and the coated-CaF_2 plate forms the sample exposure chamber. Each exposure cell contained an inlet and an outlet that allowed fresh air of the desired T and RH to continuously enter the sample exposure chamber and let the outgoing air vent to the outside of the chamber. Each exposure cell was equipped with a thermocouple and a chilled-mirror hygrometer to monitor T and RH, respectively. It should be noted here that, during the early stage of exposure, essentially no photodegradation was observed in the specimens beneath the filters. The results of these specimens were included in the analysis of hydrolysis rates. For that reason, the description of specimens under the interference filters is included in this section.

Two temperature-humidity generators, based on the principle of dry/moisture-saturated air mixture, supplied the desired relative humidities.[12] Each temperature-humidity generator was capable of providing air at one temperature and up to four different RH levels. The RH and T in each cell were controlled by a feedback system, which tracked RH and T three times per second. RH and T in each exposure cell could be independently controlled and maintained to within ± 0.5°C and ± 3%, respectively, of the preset values.

Water Sorption Measurement

Free standing film specimens from the same coating formulation having a dimension of approximately 0.15 × 3 × 6 mm were employed for water sorption measurement at different relative humidities. Free films were prepared by drawdown on poly(ethylene terephthalate) sheets attached to an aluminum substrate. Spacers were used to control the film thickness. The films were cured at 130°C for 20 min, similar to that used for the hydrolysis study. The sorption was performed in a Hidden ISAsorp Moisture Sorption Analyzer, which is equipped with a microbalance having a resolution of 1×10^{-7}g. The instrument can accurately control the environmental chamber to within ± 1% of the preset values of RH from 0 to 90% and ± 0.05°C of T from 5° to 70°C, respectively. The sorption isotherm was generated using the isothermal mapper mode. In this mode, the instrument is programmed to record the water uptake at the higher specified RH after reaching the equilibrium uptake of the lower specified RH. In the isotherm mode, only one specimen is required for the whole RH range. Before starting the adsorption process, specimens were dried at 60°C in the analyzer using the drying mode until no further decrease in the sample mass was observed. Unless otherwise stated, the results were the average of the three specimens.

Atomic Force Microscopy (AFM)

Tapping mode AFM was used to provide information on nanoscale surface microstructure and morphology of the coating before and during exposures. In AFM, a sharp tip located at the end of a cantilever beam is scanned across the sample surface. For tapping mode AFM, the cantilever is oscillated at a frequency near its resonance, typically, a few hundred kHz, so that the tip makes contact with the sample only for a short duration in each oscillation cycle. As the tip approaches the sample, the tip-sample interactions change the amplitude, resonance frequency, and phase angle of the oscillating cantilever. Monitoring changes in the amplitude and phase angle would provide the topographic (or height) image and phase image, respectively. Phase angle shift is sensitive to changes in sample properties. Therefore, phase imaging often provides significantly more contrast than topographic image and has been shown to be a useful technique for studying surface heterogeneity with nanoscale lateral resolution.[18]

AFM measurements were performed using a Dimension 3100 Scanning Probe Microscope (Digital

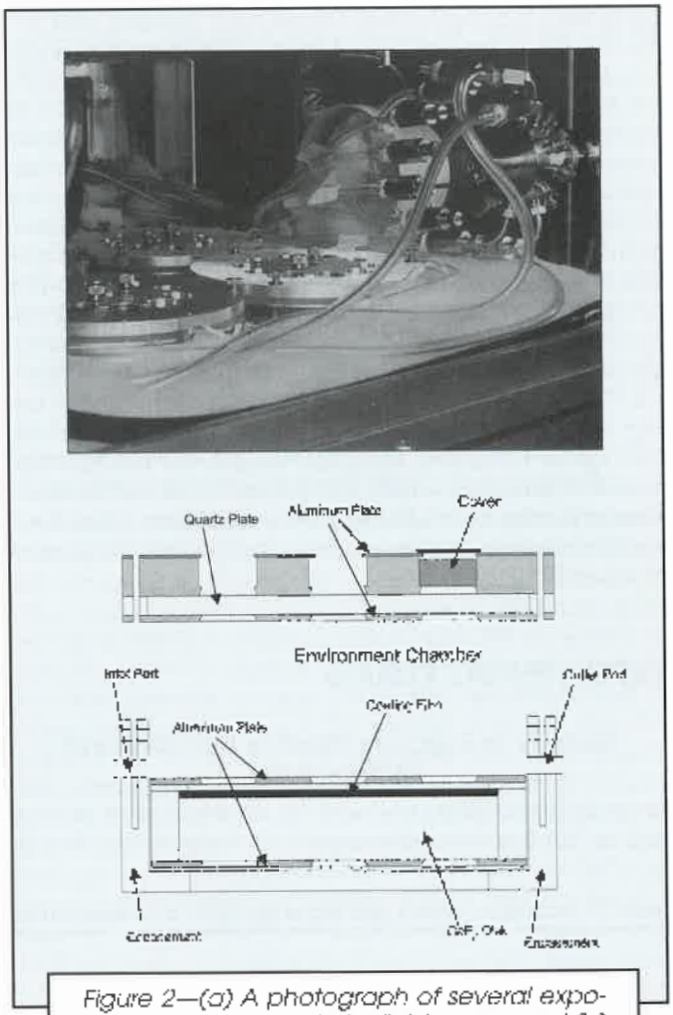

Figure 2—(a) A photograph of several exposure cells underneath the light source and (b) cross-section of an exposure cell showing the quartz plate, the coated CaF_2 and the space containing the sample exposure environment.

Instruments) under ambient conditions (24°C and 45% RH). AFM images taken during exposure were obtained from the same specimens used for FTIR analysis. A special holder was fabricated so that the 100 mm diameter coated sample could be secured repeatedly in the same orientation. AFM images were taken approximately at the same sample area for every measuring time by using a reference mark and controlling the x-y stage. More details on this procedure are described elsewhere.[19] Both topographic and phase images were taken using a tapping force of between 50 and 70% of the free amplitude. Silicon tips having a drive frequency of approximately 300 kHz and a radius of approximately 5 nm were employed.

Fourier Transform Infrared Spectroscopy Analysis

Coating hydrolysis was followed by FTIR spectroscopy in the transmission mode using an autosampling accessory. At each specified time, coated CaF_2 plates were removed from the exposure cell and fitted into a demountable 150 mm diameter ring of the autosampling device. The ring was computer-controlled and could be rotated and translated to cover the entire sampling area. Spring-loaded Delrin clips ensured that the specimens were precisely located and correctly registered. This automated sampling system allowed unattended, efficient, and speedy recording of the FTIR transmission spectra of the coating at all 12 windows before or at each exposure time. A photograph of the autosampler loaded with specimens is given in reference 11. Since the exposure cell was mounted precisely in the autosampler, error due to variation of sampling at different exposure times was essentially eliminated. The specimen-contained autosampler was placed in an FTIR spectrometer compartment equipped with a liquid nitrogen-cooled mercury cadmium telluride (MCT) detector. Spectra were recorded at a resolution of 4 cm^{-1} using dry air as the purge gas. All spectra were the average of 132 scans. The peak height was used to represent IR intensity, which is expressed in absorbance, A. Except for the << 1% RH exposure condition where four specimens were employed, only one specimen was used at other RH levels.

EXPERIMENTAL RESULTS

Stability of Exposure Relative Humidity and Temperature

Relative humidities produced by the method of mixing dry air and moisture-saturated air were stable during the course of exposure, even at elevated temperatures. The maximum coefficient of variation, i.e., (standard deviation/mean) × 100, of the five RH levels studied was 3% during the six months of exposure. The coefficient of variation for the 50°C temperature was < 1%. The RH at 0.002% (designated as << 1% or very dry) was estimated from the Table of Vapor Pressure of Water,[20] given the 50°C exposure temperature and the –70°C dew point. The RH sensor, i.e., the chilled-mirror hygrometer, was not sensitive enough to record this low RH.

Water Sorption Characteristics

Figure 3 displays the equilibrium water uptake as a function of relative humidity (sorption isotherm) at 50°C for the model acrylic-melamine coating used in this study. In this figure, the moisture contents (% equilibrium mass of water uptake with respect to the dry mass of the coating) at 50, 60, 80, and 95% RH were obtained from only one specimen. However, the data point for each of the other five RH levels was the average of three specimens. *Figure* 3 includes the one standard deviation error bars at the multiple sample data points, which show that variation between the samples is small. Equilibrium moisture contents and water solubilities of the coating at the five relative humidities used in this hydrolysis study are presented in *Table* 1. Solubility is expressed as moles of water (i.e., equilibrium mass of water uptake divided by the molecular mass of water) per 100 g dry coating film. The water vapor adsorption in these acrylic-melamine coatings is almost linear between zero and 50% RH but increases more rapidly thereafter, reaching a value of about 1.8% at 90.8% RH.

The sorption isotherm shown in *Figure* 3 provides essential information not only on the hydrolysis kinetics (a function of water concentration) but also for understanding how water sorption characteristics in an acrylic-melamine coating varies with RH change. The isotherm in *Figure* 3 is of the Type III in the BET (Brunauer, Emmett, and Teller) classification.[21] Except for the magnitude, the shape of this curve is similar to those of cellulose acetates,[22] acrylic polymers,[23] and polyamides[24] at 50°C. For this type of sorption (upward curvature), the heat of adsorption of the water vapor on an adsorbate is similar to or less than the heat of condensation of the water vapor.[21] For the acrylic-melamine material, this means that the interaction between water molecules themselves is energetically similar or greater than that between water vapor and the acrylic-melamine material. Based on the shape of the curve in *Figure* 3, it is suggested that multiplayer adsorption ("clustering") of water has occurred in this acrylic-

Table 1—Moisture Content and Water Solubility at Different Relative Humidities of the Acrylic-Melamine Coating Used in this Study

	Relative Humidity, %				
	0.002	19.2	41.7	72.7	90.8
Moisture content (%)	–0.009 ± 0.31[a]	0.23 ± 0.007	0.53 ± 0.008	1.16 ± 0.08	1.84 ± 0.06 (%)
Solubility	–0.0005 ± 0.0007	0.013 ± 0.0004	0.03 ± 0.0004	0.06 ± 0.005	0.01 ± 0.003
(Mole H_2O/100 g coating)					

(a) The number of or the ± symbol indicates one standard deviation.

melamine coating. However, the deviation from linearity (i.e., from the Henry's law behavior) of the curve in *Figure* 3, although substantial, is not radical. Such type of curves, i.e., small positive deviation from the Henry's law, generally indicates that the number of water layers adsorbed in the polymer film does not exceed the dimer level.[22,23]

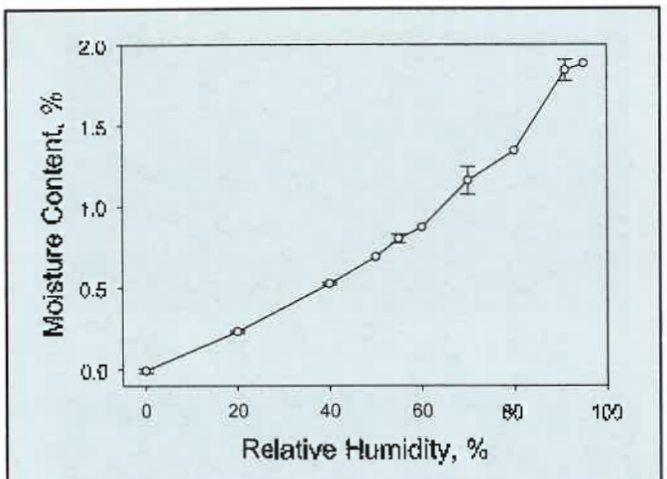

Figure 3—Sorption isotherm at 50°C for the acrylic-melamine coating (one standard deviation error bars are given for the five RH levels used in this study).

Atomic Force Microscopy

Figure 4 displays 500 nm × 500 nm topographic and phase AFM images of an approximately 50-μm thick coating before exposure. This sample was prepared by spin casting of the coating in solution on a silicon substrate. The cast film was cured using the same schedule used for FTIR analysis samples, i.e., 130°C for 20 min. The images of *Figure* 4a were taken from the surface exposed to the air (exterior), and those of *Figure* 4b were obtained from the surface that was in contact with the silicon substrate (interior) during film formation. The interior surface sample was prepared by first initiating a cut using a razor blade, followed by peeling using tweezers. It should be noted that AFM images taken at high magnification show that the silicon surface is essentially featureless, with no evidence of a surface pattern. For both *Figures* 4a and 4b, the topographic images are on the left and the phase images are on the right. The bright and dark areas in the topographic images correspond to the surface peaks and valleys, respectively. Except for the surface topographic pattern, the height images reveal little information about the microstructure of the interior or exterior surface. However, there are two characteristic features in the phase images that need to be discussed because they provide essential data for the analysis of the degradation mode.

One feature is that the acrylic-melamine coating has a two-phase microstructure (*Figure* 4b), consisting of a matrix that appears bright and interstitial regions dispersed throughout the matrix that appear dark. The 500 nm regions that were imaged were very flat, with topographic changes of less than 5 nm for both the interior and exterior surfaces. Further, there is no direct correlation between the topographic variations with dark or bright areas of the phase images. On the other hand, the phase angle difference between the bright and dark regions in the phase image of *Figure* 4b is substantial (50°). These results indicate that the property differences between the matrix and the interstitial regions of the coating are significant. High resolution AFM images of the pitted regions (i.e., microstructure beneath the outer surface layer) of this coating after exposure to UV/humid environments also showed a two-phase microstructure,[19] resembling that shown in *Figure* 4b. Further, our extensive AFM data of crosslinked amine-cured epoxies also reveal that, while the exterior surface of the epoxy samples appears featureless (similar to that observed for acrylic melamine), the two-phase microstructure of the interior surface is similar to that observed for the cryogenically fractured surfaces (bulk) and the UV-degraded regions of these materials. These results suggest that the microstructure of the interior surface (the surface that was in contact with the silicon substrate during film formation) more truly represents the microstructure of the bulk than that of the air surface. This is because the outermost layer of the outer surface is covered with a thin layer of a homogeneous low surface free energy layer, as explained later.

Phase differences between regions of a surface recorded by an AFM have been generally attributed to differences in the mechanical and/or chemical properties of those regions.[18] Softer, more compliant phases tend to be dark while harder, less viscoelastic phases tend to be bright.[25-27] Following these assignments, it is believed that the acrylic-melamine coating used in this study is a heterogeneous material consisting of softer regions (dark) dispersed in a harder matrix (bright). A similar heterogeneous microstructure has been observed by AFM for crosslinked amine-cured epoxies,[25,28] and crosslinked polyester.[29] The microstructure heterogeneity of coatings has a great implication on their degradation mode and mechanism during service.

Another feature of *Figure* 4 is the higher contrast and more well-defined microstructure of the interior surface as compared to that of the exterior surface. This difference is also indicated by a difference in the phase shift, which is only 10° for the air side but 50° for the substrate side. Such morphological differences between the interior and exterior surfaces have also been observed in other polymer systems.[26,30] It should be noted that, because AFM operates in the near field (i.e., very close to the surface), it detects only the top layer of rigidly bound atoms and, thus, does not provide an image of the layer beneath the outermost surface. Chemical analysis by X-ray photoelectron spectroscopy (XPS) of these acrylic-melamine samples shows that the exterior surface contains 66.7% C and 8.0% N, as compared to 64.8% C and 12.1% N for the interior surface. From these results, i.e., the low phase shift and less-defined microstructure (by AFM), a lower concentration of the polar N-containing groups, and a higher concentration of the low electronegativity (related directly to polarity) C element, it is suggested that the surface exposed to the air of this acrylic-melamine film is probably covered

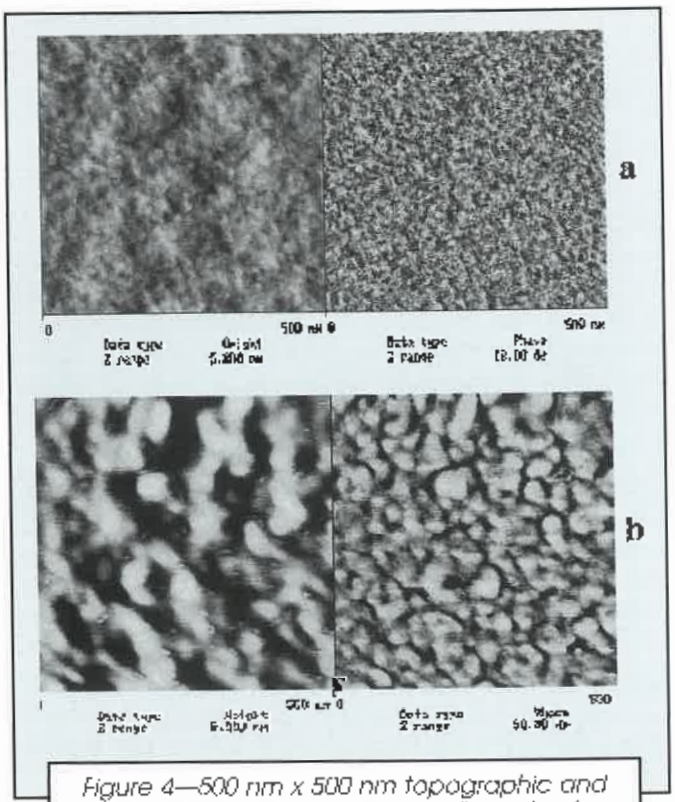

Figure 4—500 nm x 500 nm topographic and phase AFM images of the acrylic-melamine coating films: (a) exterior surface and (b) interior surface. In both a and b, the topographic image is on the left and the phase image is on the right. Contrast variation from black to white; for topographic images in both a and b: 5 nm; for the phase image: (a) 10° and (b) 50°.

with a very thin layer of a more homogeneous, lower surface-free energy material (as compared to the interior). This interpretation is consistent with extensive experimental data obtained by various surface analytical techniques showing that the air surface of a multicomponent polymer system is generally enriched with a lower surface-free-energy component to minimize polymer-air interfacial energy.[31-35]

The presence of a lower surface-free energy layer on the exterior surface should have an effect on the degradation behavior of polymer coatings. This is because, while the bulk coating underneath degrades, the more inert, hydrophobic thin layer on the exterior surface may not undergo change until much later. This is the case for the hydrolysis of the acrylic-melamine coating used in this study. While the hydrolysis is substantial after relatively short exposure time (see the FTIR results), AFM results do not reveal any evidence of surface degradation, even at nanoscale resolution, until more than 600 hr exposure (see *Figure* 5). The difference in the degradation characteristics between the exterior surface (as revealed by AFM) and the bulk (as measured by FTIR-transmission) observed in this study may explain the lack of a correlation between surface gloss loss and bulk chemical degradation reported previously for acrylic-melamine coatings.[5] Similarly, the delay in the hydrolysis of poly(sebacic anhydride) (PSA) and poly(DL-lactic acid) (PLA) blends used to control drug deliveries has been verified by XPS and AFM as due to the surface enrichment of the more hydrolytically resistant PLA in the blends.[31] Work in our laboratory also clearly showed that a layer of enriched poly(vinylidene fluoride) (PVDF) is present on the surface of PVDF/acrylic polymer blends and that this layer is responsible for the excellent UV resistance of PVDF-based coatings.[30,36]

Figure 5 presents AFM topographic images of specimens exposed to 70% RH at 50°C for 1264 hr in the absence of UV light. Pits with lateral dimensions from 10 nanometers to several micrometers formed on the surface of this coating. However, pits were detected only after 600 hr of exposure.

FTIR Analysis of Coating Hydrolysis at Different Relative Humidities

Partially alkylated melamine resins are generally composed of different compounds with different degrees of substitutions. In addition to the methoxymethyl functionality ($-CH_2OCH_3$), a partially methylated melamine resin also contains substantial amounts of amino (–NH) and methylol groups ($-CH_2OH$).[37] Many possible reactions can take place during the curing of a partially alkylated melamine resin with the hydroxy-terminated acrylic ester used in this study.[38] Therefore, a cured film of partially alkylated melamine-acrylic coatings contains a variety of groups and linkages that may affect the hydrolysis of the coatings when they are exposed to weathering conditions.

FTIR spectra recorded before and after exposure to three RH levels at 50°C for 1536 hr are displayed in *Figure* 6a. Because the films were relatively thick (~10 μm), FTIR intensities of several strong absorption bands are substantial. However, except for the high extinction coefficient (κ) C=O band at 1730 cm^{-1} (κ = 0.36), our analyses at other absorption bands of films having thicknesses from 0.1 to 10 μm showed little deviation from the Beer's absorption law. Thus, the use of relatively thick films does not affect our ability to monitor degradation quantitatively, but rather it allows us to detect and follow subtle changes in the low IR absorption groups and the appearance of new species produced during exposure.

The major bands of interest in a cured, unaged coating, prepared by reacting a hydroxy-terminated acrylic resin and a partially methylated melamine resin are the absorptions peaking near 3520 cm^{-1}, due to the OH group of the acrylic resin, near 3380 cm^{-1}, due to OH/NH groups of the melamine resin,[39] and at 1085 cm^{-1}, due to C–O–C groups. The band near 1555 cm^{-1} has been assigned to the contributions of three different groups: triazine ring, CN attached to the ring, and CH_2.[40] Another band frequently used for curing and degradation analyses of melamine-based coatings is the band at 910 cm^{-1}, due to OCH_3 and semicircle stretch.[41] The band at 1490 cm^{-1}, whose intensity decreases substantially during exposure to humid conditions with or without light, has been assigned to the CNH group of the $-NH-CH_2-NH-$ linkages.[11]

Under the curing condition used in this study (130°C for 20 min), the samples were fully cured, as evidenced

by the fact that the FTIR intensity of the bands at 910 cm^{-1} and 2825 cm^{-1} (associated with the melamine OCH_3) did not decrease further after prolonged heating at 130°C. It is obvious from *Figure* 6a (lowest curve) that the before-exposure, cured film still contained a substantial amount of unreacted OH groups of the acrylic resin (3520 cm^{-1} band) and –NH/OH (3380 cm^{-1} band) and OCH_3 groups (2825 cm^{-1} and 910 cm^{-1} bands) of the melamine resin. These groups undergo further reactions during exposure to humid environments.

Spectra recorded at a given exposure time for different RH levels (e.g., *Figure* 6a) may provide some information about the influence of moisture on the degradation. However, the effects are more clearly seen in a difference spectrum where the intensity loss or gain of certain bands or the appearance of new bands can be readily observed. Such difference FTIR spectra for samples exposed for 1536 hr at five different RH levels are presented in *Figure* 6b. These spectra were obtained by directly subtracting the spectrum of the unexposed specimen from the spectrum of the exposed specimen. Because the spectra were collected at almost the same location of the samples by the autosampler, error due to sampling at different exposure periods was minimal. In *Figure* 6b, the intensity of numerous bands in the regions from 3050 to 2750 cm^{-1} and from 1600 to 900 cm^{-1} decreases, while the intensity in the regions from 3100 to 3400 cm^{-1} and from 1710 to 1580 cm^{-1} increases. Several new bands and shoulders also appear, including those near 1705 and 1630 cm^{-1}, which are assigned to the C=O stretching of acids and NH bending of primary amines, respectively. The acid formation can also be seen in the OH stretching of carboxylic acids, which extends from 2550 to 3600 cm^{-1}. On the other hand, the 1630 cm^{-1} band assignment is consistent with those given in the literature for primary amines.[41] It should be noted that the difference FTIR spectra of the same coating exposed to condensing humidity at 50°C for 60 days (not shown) also showed similar band formation and depletion to those displayed in *Figure* 6b; that is, the formation of primary amines at 1630 cm^{-1} and carboxylic acids at 1705 cm^{-1} and the loss of ether linkages (1805 cm^{-1} band). More complete assignments, including the bands formed during degradation, are presented elsewhere.[11]

Even under very dry exposure conditions (<< 1% RH), this model coating underwent changes, as evidenced by the decreases in the intensity of the bands in the regions between 3000 and 2800 cm^{-1} and between 600 and 900 cm^{-1}. These changes were probably caused by the hydrolysis reactions during exposure to this condition. The water molecules required for this hydrolysis were probably supplied by several water-producing reactions taking place during this post-curing, including the self-condensation reactions.[36-39]

It is evident from *Figure* 6b that exposure to humid environments in the absence of UV light can produce a substantial change in various functional groups in an acrylic-melamine coating. The intensities of the bands at 1085, 1630, and 2960 cm^{-1} (CH stretching) have been chosen to follow C–O bond loss, primary amine formation, and CH loss, respectively, during exposure to different relative humidities. It should be noted that the 1085 cm^{-1} band is due to the C–O–C bond of both the acrylic-melamine crosslinks, –N–C–O–R –, and the unreacted –N–C–O CH_3 groups in the melamine chains. Acid-catalyzed hydrolysis of this type of ether is very complex,[13,15] and no attempt was made to separate the contribution of each ether type in the coating used in this study. Thus, a change in the 1085 cm^{-1} band intensity is assumed to be a sum of C–O–C concentration of both the acrylic-melamine crosslink and that of the melamine methoxy group.

Figures 7a-7c display FTIR intensity changes with exposure time at different RH levels for the C–O loss, NH_2 formation, and CH loss, respectively, of specimens exposed to 50°C in the absence of UV light. In this figure, the total intensity increase or decrease at a particular humidity is due to the sum of post-curing reactions (changes occurring at RH << 1%) and hydrolysis resulting from the reactions with water in the film at that particular RH. *Figure* 7 results show that the extent of all three degradation processes (i.e., NH_2 formation, C–O loss, and CH loss) increases with increasing RH.

Figure 8 depicts the hydrolysis rates, along with their one standard deviation error bars, as a function of RH for the three degradation processes. The rates, which are expressed as change in FTIR absorbance with exposure time (dA/dt), were taken from the data within a five-day exposure. The results at << 1% RH in *Figure* 8 were the average of four specimens, as indicated in the Experimental section. On the other hand, the rate results for each of the relative humidities from 19.2 to 90.8% were the average of 11 specimens, which included the covered (no-UV) specimen and 10 specimens under the interference filters. The results of specimens un-

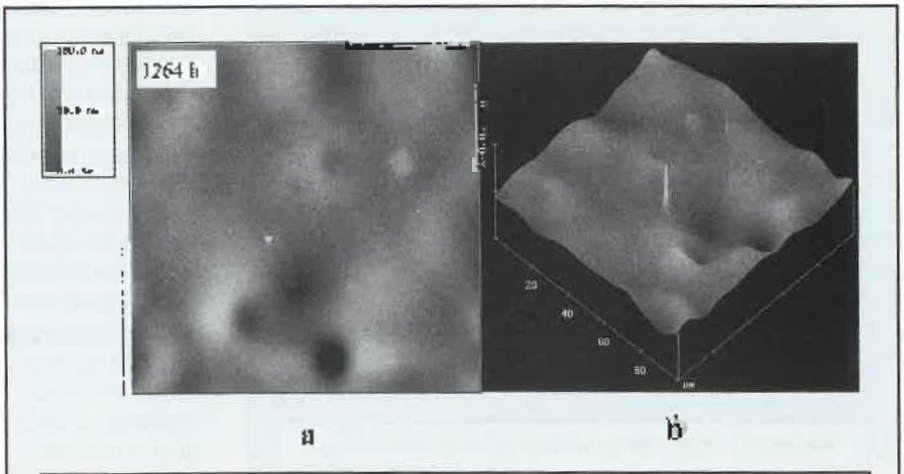

Figure 5—100 μm x 100 μm 2D (a) and 3D (b) topographic AFM images of the acrylic-melamine coating film exposed to 70% RH at 50°C for 1264 hr.

der the interference filters were included for the analysis because only hydrolysis (i.e., no photodegradation) was observed to occur on these specimens during the first five days of exposure, which was the period used for determining the hydrolysis rates. The larger error bars for the CII band are due to the small change in the IR intensity of this degradation process. The specimen exposed to the full UV condition underwent a substantial photodegradation at all RH levels, even at early exposure time,[11] and, thus, was not used for the analysis.

Except for the low RH levels (<< 1% and 19.2%), where the rate is nearly constant with time, the hydrolysis rates at other RH levels are rapid at the early exposure stage and then slow down at the long exposure times. Bauer[13] also observed a decrease in the hydrolysis rate of partially alkylated melamine-acrylic coatings at long exposure times, and attributed the decrease to the different reactivities of different methoxy groups in the melamine resin. The most reactive methoxy groups hydrolyze first and the less reactive groups are consumed later, leading to the slowing down of the reaction rate at longer exposures. *Figures* 7 and 8 show that both the rates and extents of the three degradation processes increase with increasing RH. However, the rates of NH_2 formation are greatest and those of CII consumption are lowest, among the three processes. The rate difference between the primary amine formation and the ether loss is probably due to more than one reaction taking place for the latter process, in which the crosslinked ether groups were both consumed and generated at the same time during hydrolysis (see Mechanism section).

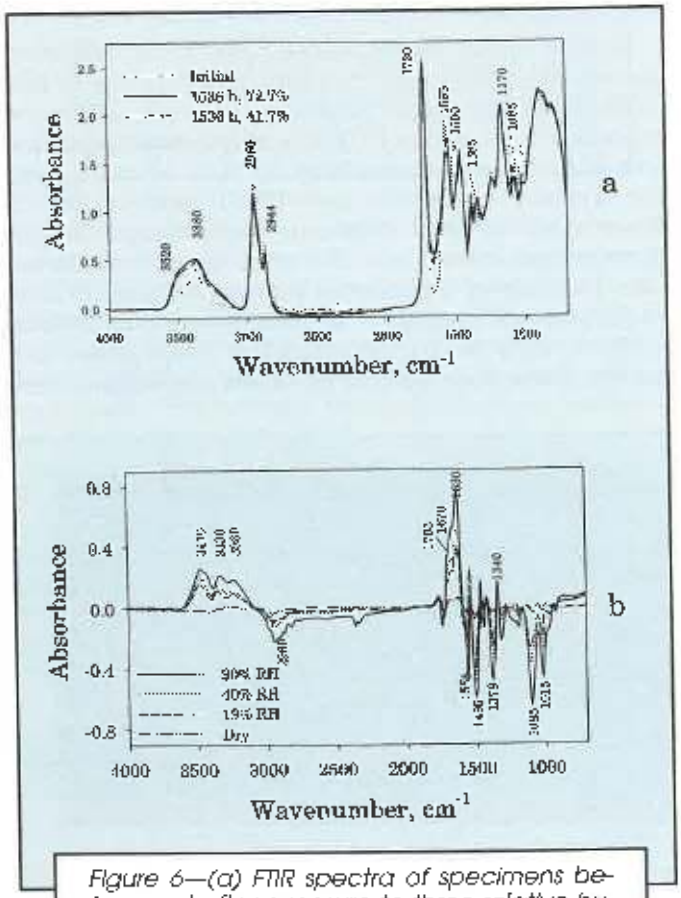

Figure 6—(a) FTIR spectra of specimens before and after exposure to three relative humidities at 50°C in the absence of light and (b) difference FTIR spectra for several RH levels at 50°C for 1536 hr.

DEGRADATION MODE

It has been generally believed that the degradation of polymeric coatings is a homogeneous process in which the loss of material is uniform across the surface of the sample. However, the AFM images shown in *Figure* 5 and other AFM results in reference 19 indicate that the degradation of an acrylic-melamine coating exposed to a humid environment in the absence of UV light is localized and inhomogeneous. Hydrolysis initiated at isolated locations followed by pitting at these initially degraded areas. The pits then deepened and enlarged with exposure time, with essentially little increase in the number of pits. The same localized degradation mode is observed on the same coating that was exposed to humidity in the presence of UV light, except that the pits are deeper and their radii are larger.[19] The same pitting phenomenon has also been observed for acid-catalyzed hydrolysis of poly(orthoester) and poly(anhydrides)[42,43] and base-catalyzed hydrolysis of polyester.[27] Similar to our result for acrylic-melamine coatings, AFM results of these studies showed that pits are formed at certain sites; pits then enlarge and deepen from these sites. And finally, pit formation at the nanometer to micrometer sizes detected by AFM at the early hydrolysis stages for this material is similar to the natural etching (pitting) reported for acrylic-melamine coatings exposed to acid rain environments or acid rain-rich outdoor locations.[1,3,4]

Localized degradation seen in the AFM images shown in *Figure* 5 supports our belief that hydrolytic degradation of an acrylic-melamine coating initiates at the hydrophilic (as defined in the following discussion) areas of the film. The hydrolysis then expands from these areas following an autocatalytic process. This postulation is consistent with the fact that both the water uptake and the diffusion rate of water in a highly crosslinked material or region are low and that hydrolysis reactions of organic compounds in a neutral environment are very slow. This conjecture is similar to that proposed by Nguyen et al.[44] for the formation of conductive pathways in polymer coatings on steel during exposure to electrolytes. Such conductive pathways, which are also believed to develop in the hydrophilic, water-susceptible regions of the coatings, are responsible for the direct transport of ions from the environment to the metal surface, leading to accelerated corrosion of metals protected by an intact organic coating.

The inhomogeneous degradation mode may be explained by the heterogeneous microstructure of this material as shown in *Figure* 4 and of a variety of organic coatings, which have been well documented. Karyakina and Kuzmak[45] have reviewed and discussed in detail heterogeneity of polymers and coatings and have concluded that polymer coatings generally consist of microgels connected via a spatial network. Bascom[46] has proposed that heterogeneity in polymers is formed

because, as the high molecular mass segments polymerize and terminate to form a network, some unreacted and partially polymerized materials are unable to merge into the homogeneous structure and are left at the periphery of the network units. Early microscopic studies of epoxy, phenolic, and phthalate resins revealed that the microstructure of these materials is not homogeneous but is comprised of high-density nodules separated by narrow interstitial regions of lower molecular mass material.[47-50] For thermoset epoxy, the interstitial regions behave like a liquid material,[47] and the volume fractions of the two regions can be estimated by modeling.[50] Such two-phase structures for a variety of amine-cured epoxies and a polyester are clearly evident from recent high lateral resolution AFM phase imaging studies.[25,26,51] The first direct chemical evidence of inhomogeneity in a thermoset film was provided by a recent investigation using a high-resolution near infrared multispectral imaging technique.[52] This study showed that the reaction rates within an epoxy sample are very inhomogeneous and the difference in the degree of cure at different locations can be as high as 37%.

The most intensive study of film heterogeneity and how it affects the protective performance of organic coatings was performed by Mayne and his coworkers.[53-55] Using microhardness and DC resistance measurements, they have identified a "conducting polymer phase," which they termed D type, in a variety of coating films. The D type regions are softer, swell more, and have a lower crosslinking density than the rest of the film. Corrosion of organic-coated steel has been observed directly beneath the D type regions. Mills and Mayne postulated that the D type regions are formed by partially polymerized or "dead" molecules, which are present in the resin before casting. During curing, these molecules congregate, and due to their low functionality, do not crosslink to the same extent as the rest of the film.[55] The water sorption and transport characteristics of the D areas have been found to be similar to those of a hydrophilic, ion-exchanged membrane[56,57]; that is, they take up a large amount of water (45-75%) and have a high ion diffusion coefficient. The existence of the low resistance, D type regions in phenolic, polyurethane, and alkyd coatings has been confirmed by array electrode technique.[58] A water extraction study also showed that cured films of alkyd and epoxy ester lose about 4-5% of their initial mass,[59] clearly indicating that these coatings contain low molecular mass, water-soluble materials.

All these referenced studies point to a conclusion that most, if not all, thermoset coatings are inhomogeneous materials consisting of low molecular mass, low crosslink, and soft regions (designated as hydrophilic regions) dispersed in a highly crosslinked network structure. During exposure to aggressive environments, pores or pits are believed to initiate and develop in the hydrophilic regions of the films. Direct evidence to support the view that pit formation starts at the hydrophilic regions is from a recent study of hydrolyzable/nonhydrolyzable polymer blends exposed to hydrolytic environments.[60] AFM images of this study clearly showed that pits initiate and develop at the locations occupied by the hydrolyzable polymer. The postulation that polymeric coatings consist of hydrophilic regions dispersed

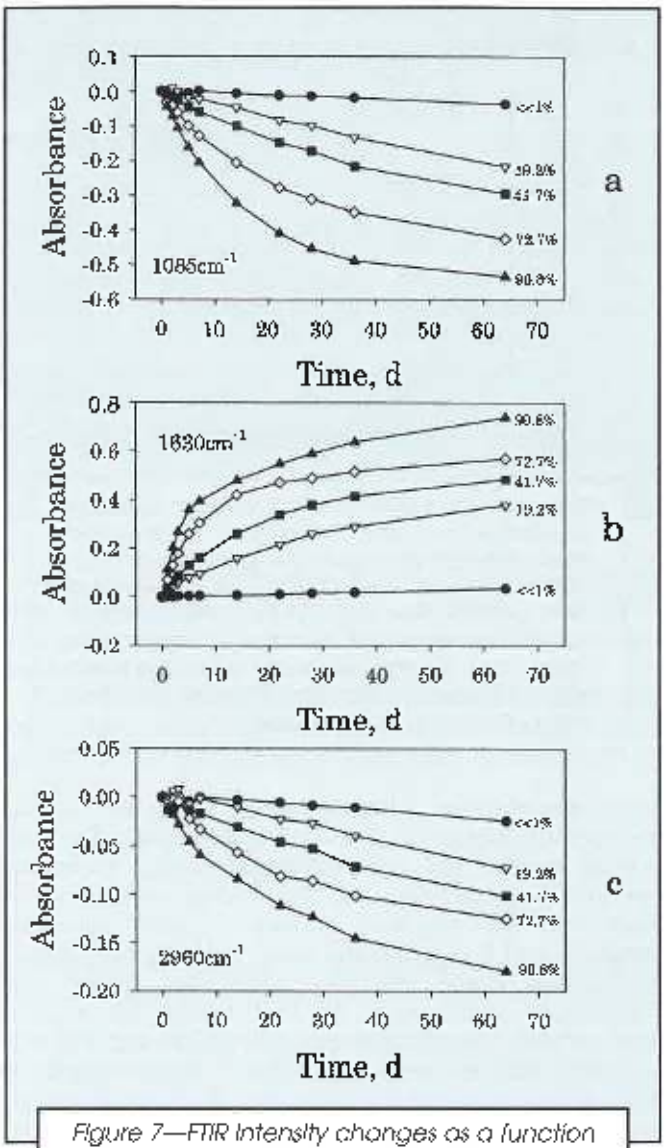

Figure 7—FTIR intensity changes as a function of exposure time for five RH levels at 50°C in the absence of light: (a) C–O band at 1085 cm⁻¹, (b) NH_2 band at 1630 cm⁻¹, and (c) CH band at 2960 cm⁻¹.

in a crosslinked network and that hydrolytic degradation mostly occurs in the hydrophilic regions is also experimentally demonstrated by scanning electron microscopy (SEM), small angle neutron scattering (SANS), and transmission electron microscopy (TEM) studies.[45,59] For example, SEM results obtained during water sorption in a number of crosslinked polymers clearly showed that water does not diffuse uniformly in these materials, but in regions along the boundaries of the network units.[45] Similarly, SANS and TEM results clearly revealed that the hydrophilic carboxylic acid compounds in carboxylated styrene-butadiene latex films mostly concentrate at the particle-particle interface and that water transport in these latex films is mainly along the hydrophilic interface, and not through the crosslinked particles.[59]

For acrylic-melamine coatings, such an heterogeneous structure is schematically illustrated in *Figure* 9, which shows hydrophilic (hydrolysis-susceptible) re-

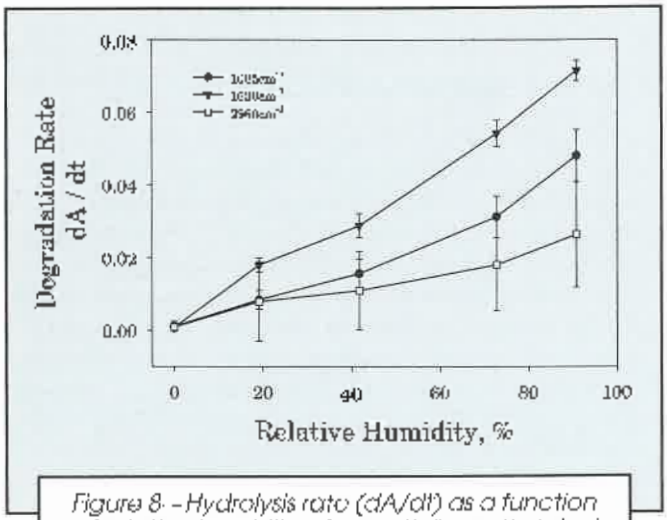

Figure 8 – Hydrolysis rate (dA/dt) as a function of relative humidity of a partially methylated melamine-acrylic coating exposed to 50°C in the absence of UV light for C–O loss, primary amine formation, and CH loss. (The results at << 1% RH were the average of four specimens and at other RH levels were the average of 11 specimens; and the error bars indicate one standard deviation.)

gions dispersed in a highly crosslinked network. The hydrophilic regions in this coating are believed to consist of hygroscopic compounds, including melamine methylols and acrylic acid, and hydrolysis-susceptible materials, such as low molecular mass melamine methoxy and low molecular mass, partially crosslinked molecules. Since the low molecular mass, low crosslinked molecules in the hydrophilic regions contain a variety of polar groups, such as OH and NH, it is expected that these groups exist in these regions as highly hydrogen bonded molecules. In *Figure* 9, the hydrogen bonds are represented by the dotted lines connecting the electronegative O and N atoms with the hydrogen atoms. During exposure to humid environments, water enters the acrylic-melamine films predominantly at the hydrophilic sites, probably through both concentration-gradient diffusion and osmotic-driven transport. The latter process is due to the presence of hygroscopic materials. Hydrolysis then takes place in the hydrophilic regions, forming the initial pit sites.

The proposed chemically heterogeneous structure of acrylic-melamine coatings shown in *Figure* 9 is consistent with the concept advocated by Bascom[40] and Mayne[53-55] that the low molecular mass, low density, partially crosslinked materials that are responsible for the loss of protection of organic coatings during exposure to electrolytes are located at the periphery of the crosslinked units. On the other hand, the postulation that hydrolysis is more likely to take place in the low molecular mass, partially crosslinked, hydrophilic regions, and not in the highly crosslinked network, is strongly supported by Berge et al.[15] hydrolysis studies of alkoxy melamine compounds in solutions. They reported that, in mild acid conditions, the ether group of a monosubstituted amino (NH CH_2OR), which is similar to the partially crosslinked chains in an acrylic-melamine coating, hydrolyze rapidly. However, the ether groups of a disubstituted amino (ROH_2C N- CH_2OR), which is similar to the fully crosslinked structure of an acrylic-melamine coating, undergo little hydrolysis in mild acid conditions.

As indicated earlier, the exterior surface of this coating is probably covered with a thin layer of a lower surface-free energy material to minimize the polymer-air interfacial energy. The fact that AFM images reveal pit formation and development suggests that the exterior surface of this coating probably underwent a rearrangement during exposure to humid environment, schematically displayed in *Figure* 10. The phenomenon of a hydrophobic surface enrichment, which subsequently undergoes radical surface rearrangement when changing the contact medium from air to water is commonly observed for many polymers, including polyurethanes and polyamines[25,62]; a brief review on the subject is given in reference 35. The apparent driving force for the surface rearrangement is the formation of a water-hydrophilic interface. According to *Figure* 10, a thin low surface-free energy layer initially covers the outer surface of the acrylic-melamine coating film. When this coating is exposed to a humid / water environment, the thin hydrophobic layer on top of the hydrophilic regions becomes unstable and ruptures (dewetting).[35] The dewetting continues with exposure, gradually exposing the hydrophilic regions of the film to the water vapor environment. Pits initially form at these exposed hydrophilic regions, as illustrated in *Figure* 10. It is noted that, except for a difference in the composition and distribution of the hydrophilic material, the scheme shown in *Figure* 10 is similar to that proposed by Tezuka et al.[35] for the rearrangement of the polystyrene-enriched layer on the surface of polystyrene (PS)-poly(vinyl alcohol) (PVA) block copolymers when these materials are exposed to water.

It is easy to comprehend why hydrolysis reactions initiate at the hydrolysis-susceptible regions of the film. However, this could not explain why the degradation expands from these initially hydrolyzed locations, as observed in this and other studies,[42,43] instead of forming new sites. We believe that the deepening and broadening of the pits is a result of an acid autocatalyzed hydrolytic process taking place at the initiated pit sites, where the increased acidity is provided by the hydrolysis products. Substantiation for the pit deepening of acrylic melamine being an autocatalytic process comes from two sources. First, the band at 1705 cm^{-1}, due to C=O of carboxylic acids, in the spectrum shown in *Figure* 5b indicates that acids were generated during the hydrolysis of this coating (see the Mechanism section for the reactions). Second, the increased acidity in pores and pits formed during hydrolysis of other polymers has been measured.[42] Using a pH-sensitive dye in combination with fluorescence scanning confocal microscopy, this study obtained a pH of 5.7 at a depth of approximately 200 μm in the pits formed on the surface of polyanhydrides, as compared to a pH of 7.5 for the exposed solution.

It is likely that the acidity within the pits of acrylic-melamine coatings is high, as evidenced by the high in-

tensity of the 1705 cm^{-1} band for RH levels from 19.2 to 90.8% (*Figure* 6b). We believe that the high acidity generated by the hydrolysis reactions in the degraded areas accelerates the rate of hydrolysis in the pits, and that this harsh environment attacks the nearby polymer chains. This autocatalytic activity explains the deepening and enlargement of the existing pits, rather than formation of new pits, with exposure time. Autocatalytic hydrolysis has also been attributed as the main reason for the pit deepening and enlargement in other polymer systems.[42]

Other contributors to the pit deepening and broadening include the penetration of acids generated during hydrolysis into the polymer matrix. For example, the rate of poly(orthoester) erosion was reported to depend strongly on the types of acids.[60] In hydrophilic acids, such as HCl, the hydrolysis reactions were observed to occur only on the sample surface. But the hydrolysis rate in the presence of hydrophobic acids, such as perchloric acid, increased many fold, and the attacks were both on the surface and beneath the surface. Another contributing factor may be the rate of water transport to the reaction sites. Hydrolysis is a bimolecular reaction in which water and the labile functional groups are involved. Therefore, the reaction rate is determined by the concentration of both reactants, i.e., the more water there is present in the reaction zones the higher is the reaction rate. Since the pitting areas contain mostly polar materials, e.g., short chain starting compounds and hydrolysis products, they likely attract a high amount of water into these areas and, thus, increase the degradation rates. Finally, in order for pits (holes) to form in the sample, as shown in *Figure* 5, the hydrolysis products must decompose to form gases or diffuse away from the pit sites. The overall degradation rate at the pits is, therefore, controlled by a number of complex factors, including the pH in the pits, the types and molecular masses of hydrolyzable molecules, polymer microstructure, rate of water transport into the pits, and the rate at which degradation products are removed from the pits.

Information on the degradation mode and the nature of the regions where hydrolysis reactions occur should help to design more hydrolytically stable coatings. The mode of degradation proposed in this study, which is based mainly on the experimental evidence of nanoscale coating microstructure, extensive literature of corrosion of polymer-coated steel, and knowledge of polymer degradation chemistry, is preliminary. Hopefully, future research on chemical identification and characterization at nanoscale of the heterogeneous domains and degraded regions of coatings will provide a more definitive understanding on the mode of hydrolytic and other types of coatings degradation.

MECHANISM

FTIR spectral results given in *Figure* 6b show that the hydrolysis of a partially methylated melamine acrylic coating result in, among others, loss of the ether bonds (C–O at 1085 cm^{-1} band) and formation of primary amines (NH_2 at 1630 cm^{-1} band) and carboxylic acids (C=O at 1705 cm^{-1} band). The pathways responsible for the depletion of the C–O loss probably occur by the following reactions[13,15]:

1) $Tr\text{--}NH\text{–}CH_2\text{–}O\text{–}CH_3 + H_2O \rightarrow Tr\text{–}HN\text{–}CH_2OH + CH_3OH$
(I)

2) $Tr\text{--}NH\text{–}CH_2OR + H_2O \rightarrow Tr\text{–}HN\text{–}CH_2\text{–}OH + ROH$
(II)

where Tr is the triazine ring, R is the acrylic resin chain, and the compounds in the left hand side of reactions 1 to 2 (structures I and II) are the polymer chains present in the cured film, as shown in *Figure* 1.

Reactions 1 and 2 proceed by protonation of the ether oxygen atom to form melamine methylols. Disubstituted amino chains (secondary ether), such as structures III and IV,

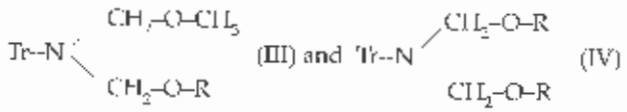

which are abundant in the film, as shown in *Figure* 1, also undergo hydrolysis to form two methylol groups per

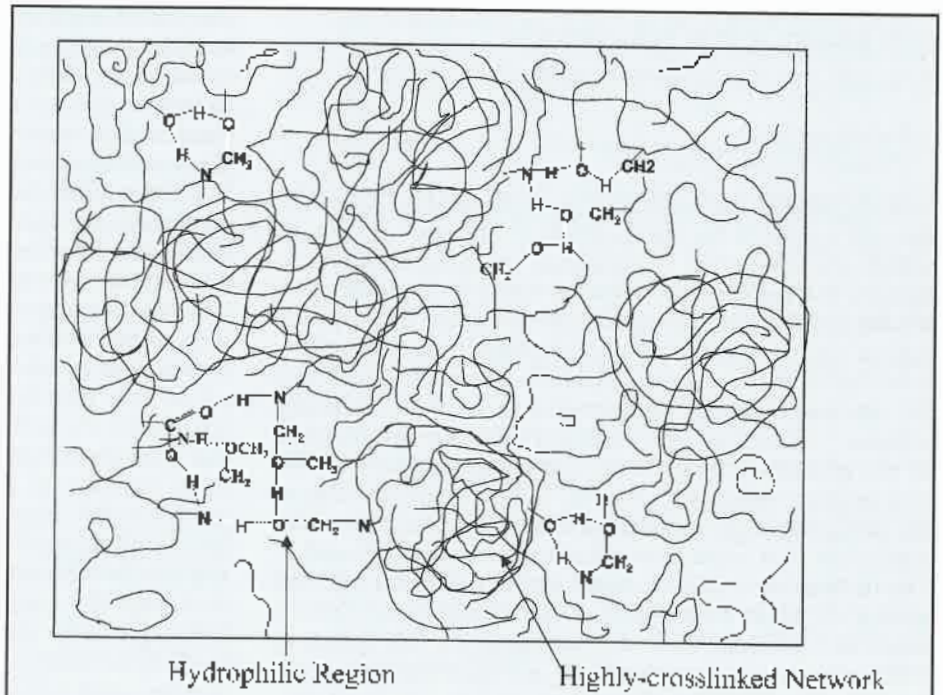

Figure 9—A schematic presentation showing the hydrophilic regions and crosslinked network for a partially methylated melamine-acrylic coating.

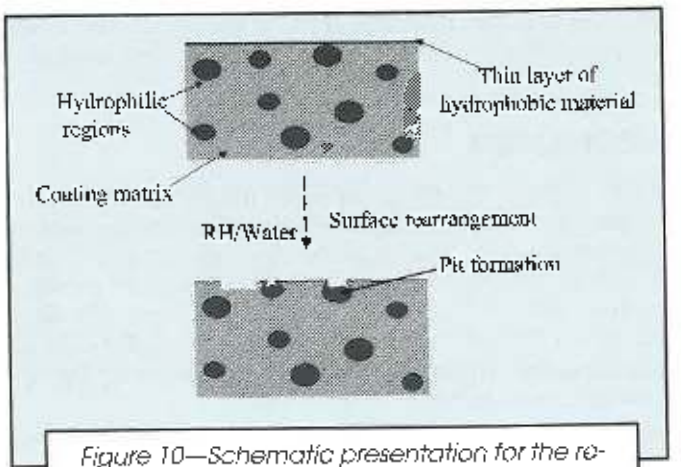

Figure 10—Schematic presentation for the rearrangement of the thin low-surface free energy layer, on the exterior surface of a partially methylated melamine-acrylic coating exposed to water vapor.

melamine chain.[15] However, because of the hydrogen on the N atom, monosubstituted amino chains (primary ether) of melamines (i.e., structures I and II) hydrolyze 30 to 40 times faster than disubstituted amino chains.[9,15] Since the hydrolysis rates of monosubstituted amino chains are much greater than those of disubstituted amino chains, it is reasonable to conclude that the rapid loss of the C–O bonds at 1085 cm^{-1} bands at the early exposure stage shown in *Figures* 6 and 7 was due mainly to the reactions 1 and 2.

The appearance of the primary amine band at 1630 cm^{-1} probably follows the pathways shown in reaction 3, where the melamine methylols generated in reactions 1 and 2, being primary alcohols, deformylate readily to form primary amines and aldehydes[15]:

3) Tr–HN–CH_2–OH (from Rx 1 and 2) $\xrightarrow[\text{fast}]{}$ Tr–NH_2 + CH_2O
(Primary amine, 1630 cm^{-1})

In this case, the methylol group is activated by the addition of a proton to the N-atom in the side group to which the methylol is attached. Since formaldehyde formed in the exposure chamber was either removed or readily oxidized to form acids (see reactions 4 and 5), reaction 3 is irreversible. The disubstituted amino methylols (that is, the hydrolysis products of structures III and IV) do not undergo deformylation to form primary amines.[15] Therefore, the intensity increase attributable to the primary amines formed during exposure in humid environments (e.g., *Figure* 7) was essentially due to the deformylation of monosubstituted amino melamine methylols that were generated from reactions 1 and 2. The formation of volatile methanol in reaction 1 and the escape of some formaldehyde molecules produced in reaction 3 probably account for most the CH losses at 2960 cm^{-1} during hydrolysis of acrylic-melamine coatings observed in *Figure* 7c.

The methylols formed in reactions 1 and 2 can also self-condense to form melamine-melamine linkages.[13] However, we believe that reaction 3 was the main pathway in the absence of UV radiation for this model coating. This is clearly demonstrated by the substantial increase of the primary amine band at 1630 cm^{-1} (*Figures* 6b and 7b) and very small increase in intensity of the band at 1550 cm^{-1} (*Figure* 6b), due to melamine-melamine linkage.[13] The 50°C temperature used in this study should accelerate this reaction, i.e., reaction 3.

The formation of carboxylic acids, as observed by the band at 1705 cm^{-1}, probably occur by the following reactions[64]:

4) $2CH_2O + O_2 \rightarrow 2HCOOH$ (formic acid, 1705 cm^{-1}).

The initial oxidation product is a peroxycarboxylic acid (HCO–OOH), which reacts readily with another formaldehyde to yield two molecules of formic acid. In the presence of water, acids may be formed by the pathway[65]:

5) $CH_2O \underset{H_2O}{\leftrightharpoons} CH_2(OH)_2 \xrightarrow[\text{fast}]{[O]} HCOOH$

Reaction 5, which is fast, may be favored inside the pits because of the hygroscopic characteristics of the compounds in these locations, which adsorb much more water than the material outside the pits. Another source of acid formation is hydrolysis of the ester groups that were formed by the reaction between the acrylic acid and the hydroxy-terminated acrylic resin taking place during curing. The ester formation is clearly seen by FTIR spectroscopy.[7]

A number of pathways for the hydrolysis of acrylic-melamine coatings, several of which produce amines has been presented previously.[13] However, the formation of primary amines and acids has not been discussed.

SUMMARY AND CONCLUSIONS

Acrylic-melamine resins are widely used for automobile exterior coatings. However, these materials are known to be susceptible to hydrolysis. Despite extensive research on etching and hydrolysis, there is little information on the mode of degradation for the hydrolysis of these materials exposed to water vapor in the absence of UV light. This study presented the mode and specific pathways for the hydrolytic degradation of a partially methylated melamine-acrylic coating exposed to different relative humidities in the absence of UV light. The coating was prepared by reacting a partially methylated melamine resin and a hydroxy-terminated acrylic resin. Samples of cured film on a CaF_2 substrate were subjected to five different RH levels ranging from approximately << 1% to 90.8% at 50°C for more than 60 days using specially designed exposure cells. Coating degradation as a function of exposure time was measured using transmission Fourier transform infrared spectroscopy and tapping mode atomic force microscopy. The following conclusions are made:

(a) In the presence of moisture and without UV light, partially methylated melamine-acrylic coatings hydrolyze quite rapidly, resulting in considerable material loss and formation of various functional groups in the film.

(b) The rate of hydrolysis, which increases with increasing RH, is rapid at the early stage and slows down at long exposure time.

(c) Hydrolysis of the crosslinks and melamine methoxy groups from monosubstituted amino chains are primarily responsible for the degradation of partially methylated melamine-acrylic coatings exposed to moist environments in the absence of light. Disubstituted amino chains (i.e., fully alkylated melamine chains) hydrolyze very slowly and contribute little to the hydrolytic degradation.

(d) The primary products formed during hydrolysis in the absence of UV light are primary amines and formic acid. Primary amines are formed by the deformylation of monosubstituted amino methylols produced by the hydrolysis, and formic acids are generated by oxidizing formaldehydes generated by the methylol deformylation.

(e) Hydrolytic degradation is an inhomogeneous process where pits, which form locally, deepen and enlarge with exposure time. Such localized degradation is a result of an autocatalytic process in which acidic hydrolysis products accumulated in the pits catalyze and accelerate the hydrolysis reactions.

Information on the specific mechanism and mode for the hydrolytic degradation of acrylic-melamine coatings is essential for understanding the controlling factors responsible for the failures and for developing accurate methodologies to predict the service life of these coatings. Further, a clear understanding of the nature of the regions where hydrolysis occurs and of the ensuing degradation process as offered in this study should help to design more hydrolytically resistant coatings.

ACKNOWLEDGMENTS

The research reported here is part of a government/industry consortium on Service Life Prediction of Coatings at NIST. Companies involved in this consortium include AKZO Nobel, ATOFINA, Atlas Material Testing Technology LLC, The Dow Chemical Company, DuPont Automotives, Duron Inc., Eastman Chemicals, Millennium Inorganic Chemicals, PPG industries, Inc., and Sherwin Williams Co. Federal Highway Administration, Air Force Research Laboratory, and USDA Forest Service (Forest Products Laboratory) also provided additional funds for this research. We also thank Drs. Xiaohong Gu and Mark VanLandingham for their AFM measurements, and Dr. Diep Nguyen, of PPG Industries, for XPS analysis assistance.

References

(1) Schmitz, P.J., Holubka, J.W., and Xu, L., "Acid Etch of Automotive Clearcoats II. Comparison of Degradation Chemistry in Laboratory and Field Testing," JOURNAL OF COATINGS TECHNOLOGY, *72*, No. 902, 53 (2000).
(2) Holubka, J.W., Schmitz, P.J., and Xu, L-F., "Mechanism for Environmental Etch of Acrylic Melamine-Based Automotive Clearcoats: Identification of Degradation Products," JOURNAL OF COATINGS TECHNOLOGY, *72*, No. 904, 39 (2000).
(3) Schulz, U., Trubiroha, P., Schernau, U., and Baumgart, H., *Prog. Org. Coat.*, 40, 151 (2000).
(4) Rogers, W.R., Garner, D.P., and Cheever, G.D., "Study of the Attack of Acidic Solutions on Melamine-Acrylic Basecoat/Clearcoat Paint Systems," JOURNAL OF COATINGS TECHNOLOGY, *70*, No 877, 83 (1998).
(5) Wernstäh, K.L., *Polym. Deg. Stab.*, 54, 57 (1996).
(6) English, A.D. and Spinelli, J.J., "Degradation Chemistry of Primary Crosslinks in High Solids Enamel Finishes: Solar Assisted Hydrolysis," JOURNAL OF COATINGS TECHNOLOGY, *56*, No. 711, 43 (1984).
(7) Bauer, D.R. and Briggs, L.M., in *Characterization of Highly Crosslinked Polymers*, Labana, S.S. and Dickie, R.A. (Eds.), *ACS Symposium Series 243*, American Chemical Society, Washington, D.C., p. 271, 1983.
(8) Bauer, D. and Mielewski, D.F., *Polym. Deg. Stab.*, 40, 349 (1993).
(9) Gerlock, J.L., Van Oene, H., and Bauer, D., *Euro. Polym. J.*, 19, 11 (1983).
(10) Gerlock, J.L., Dean, M.J., Korniski, T.J., and Bauer, D.R., *Ind. Eng. Chem. Prod. Res. Dev.*, 25, 449 (1986).
(11) Nguyen, T., Martin, J., Byrd, E., and Embree, N., "Relating Laboratory and Outdoor Exposure of Coatings: II. Effects of Relative Humidity on Photodegradation and the Apparent Quantum Yield of Acrylic-Melamine Coatings," JOURNAL OF COATINGS TECHNOLOGY, *74*, No. 932, 65 (2002).
(12) Nguyen, T., Martin, J.W., Byrd, E., and Embree, N., *Polym. Deg. Stab.*, 77, 1 (2002).
(13) Bauer, D.R., *J. Appl. Polym. Sci.*, 27, 3651 (1982).
(14) Berge, A., Gudmunsen, S., and Ulgelstad, J., *Eur. Polym. J.*, 5, 171 (1969).
(15) Berge, A., Kvaeven, and Ugelstad, J., *Eur. Polym. J.*, 6, 981 (1970).
(16) Rancourt, J.D., *Optical Thin Films*, User's Handbook, McGraw-Hill, New York, Chap. 6, p. 183, 1987.
(17) Martin, J.W., Nguyen, T., Byrd, E., Embree, N., and Dickens, B., *Polym. Deg. Stab.*, 75, 193 (2002).
(18) Magonov, S.N. and Heaton, M.G., *Am. Laboratory*, 30, May (1998).
(19) VanLandingham, M., Nguyen, T., Byrd, E., and Martin, J.W., "On the Use of the Atomic Force Microscopy to Monitor Physical Degradation of Polymeric Coating Surfaces," JOURNAL OF COATINGS TECHNOLOGY, *73*, No. 923, 43 (2001).
(20) Weast, R. (Ed.), *Handbook of Chemistry and Physics*, CRC Press, 53rd ed., p. D 148, 1972.
(21) Adamson, A.W., *Physical Chemistry of Surfaces*, Interscience, New York, 2nd ed., pp. 584-589, 1967.
(22) Barrie, J.A. and Machin, D., *Trans Faraday Soc.*, 67, 244 (1971).
(23) Toprak, C., Agar, J.N., and Falk, M., *J. Chem. Soc. Faraday*, 75, 803 (1979).
(24) Barrie, J.A., in *Diffusion in Polymers*, Crank, J. and Park, G.S. (Eds.), Academic Press, New York, pp. 259-308, 1968.
(25) VanLandingham, M.R., Eduljee, R.F., and Gillespie, J.W., Jr., *J. Appl. Polym. Sci.*, 71, 669 (1999).
(26) Magonov, S.N., Elings, V.B., and Papkov, V.S., *Polymer*, 38, 297 (1997).
(27) Sauer, B.B., McLean, R.S., and Thomas, R.R., *Langmuir*, 14, 3045 (1998).
(28) Giraud, M., Nguyen, T., Gu, X., and VanLandingham, M., *Proc. Adhesion Society Meeting*, Emerson, J.A. (Ed.), p. 260, 2001.
(29) Gu, X., Raghavan, D., Nguyen, T., and VanLandingham, M., *Polym. Deg. Stab.*, 74, 139 (2001).
(30) Nguyen, T., Gu., X., VanLandingham, M., Giraud, M., Dutruc-Rosset, R., Ryntz, R., and Nguyen, D., *Proc. Adhesion Society Meeting*, Emerson, J.A. (Ed.), p. 68, 2001.
(31) Hearn, M.J., Ratner, B.D., and Briggs, D., *Macromolecules*, 21, 2950 (1988).
(32) Yoon, S.C., Ratner, B.D., Iván, B., and Kennedy, J.P., *Macromolecules*, 27, 1548 (1994).
(33) Shakesheff, K.M., Evora, C., Soriano, I., and Langer, R., *J. Colloid Interface Sci.*, 185, 538 (1996).
(34) Chen, X., McGurk, S.L., Davies, M.C., Roberts, C.J., Shakesheff, K.M., Tendler, S.J.B., and Williams, P.M., *Macromolecules*, 31, 2278 (1998).
(35) Pienka, Z., Oike, H., and Tezuka, Y., *Langmuir*, 15, 3197 (1999).
(36) Gu, X., Nguyen, T., Sung, L., and Jean, J., *Proc. of the Federation of Societies for Coatings Technology Annual Meeting Program*, New Orleans, LA, November, 2002.
(37) Chang, T.T., *Prog. Org. Coat.*, 29, 45 (1996).
(38) Blank, W.J. and Hensley, W.L., "Use of Amino Crosslinking Agents in Water-Based Coatings," JOURNAL OF PAINT TECHNOLOGY, *46*, No. 593, 56 (1974).
(39) Bauer, D. and Dickie, R., *J. Appl. Polym. Sci.*, 18, 2014 (1980).
(40) Larkin, P.J., Makowski, M.P., Colthup, N.B., and Flood, L.A., *Vibrational Spectros.*, 17, 53 (1998).

(41) Colthup, N.B., Daly, L.H., and Wiberley, S.E., *Introduction to Infrared and Raman Spectroscopy*, 3rd ed., Academic Press, New York, p. 439, 1990.
(42) Leadley, S.R., Shakesheff, K.M., et al., *Biomaterials*, 19, 1353 (1998).
(43) Copterich, A. and Langer, R., *J. Polym. Sci., Part A, Polym. Chem.*, 31, 245 (1993).
(44) Nguyen, T., Hubbard, J.B., and Pommersheim, J.M., "Unified Model for the Degradation of Organic Coatings on Steel in a Neutral Electrolyte," JOURNAL OF COATINGS TECHNOLOGY, 68, No. 855, 45 (1996).
(45) Karyakina, M.I. and Kuzmak, A.E., *Prog. Org. Coat.*, 18, 325 (1990).
(46) Bascom, W.D., *J. Adhesion*, 2, 168 (1970).
(47) Cuthrell, R.E., *J. Appl. Polym. Sci.*, 12, 1263 (1968).
(48) Irath, E.H. and Robinson, M., *Proc. Am. Chem. Soc. Meeting, Organic Coatings and Plastics Division*, 23, 395 (1963).
(49) Racich, J.L. and Koutsky, J.E., in *Chemistry and Properties of Crosslinked Polymers*, Labana, S.S. (Ed.), Academic Press, p. 303, 1977.
(50) Kontou, E., Spathis, G., and Theocaris, P.S., *J. Polymer Sci., Polym. Chem.*, 23, 1493 (1985).
(51) Gu, X., Nguyen, T., Vant andingham, M., and Raghavan, D., *Proc. Adhesion Society Meeting*, Orlando, pp. 537-539, February 2002.
(52) Fischer, M. and Tran, C.D., *Anal. Chem.*, 71, 953 (1999).
(53) Mayne, J.E.O. and Scantlebury, J.D., *Br. Polymer*, 2, 240 (1970).
(54) Mayne, J.E.O. and Mills, D.J., *J. Oil & Colour Chemists' Assoc.*, 58, 155 (1975).
(55) Mills, D.J. and Mayne, J.E.O., in *Corrosion Control by Organic Coatings*, H. Leiheiser, Jr. (Ed.), National Association of Corrosion Engineers, Houston, TX, p. 12; and references therein, 1981.
(56) Fernandez-Prini, R. and Corti, H., "Epoxy Coal Tar Films: Membrane Properties and Film Deterioration," JOURNAL OF COATINGS TECHNOLOGY, 49, No. 632, 62 (1977).
(57) Corti, H., Fernandez, P.R., and Gomez, D., *Prog. Org. Coat.*, 10, 5 (1982).
(58) Wu, C.L., Zhou, X.J., and Tan, Y.J., *Prog. Org. Coat.*, 25, 379 (1995).
(59) Walker, P., *Official Digest*, 37, No. 491, 1561 (1965).
(60) Raghavan, D., Gu, X., Van Landingham, M., and Nguyen, T., *J. Polym. Sci., Polymer Physics*, 39, 1460 (2001).
(61) Richard, J. Mignaud, C., and Wong, K., *Polym. Inter.*, 30, 431 (1993).
(62) Tesuka, Y., Nobe, S., and Shiomi, T., *Macromolecules*, 28, 8251 (1995).
(63) Nguyen, T.H., Himmelstein, K.J., and Higuchi, T., *J. Controlled Rel.* 4, 9 (1986).
(64) Streitwieser, D. Jr. and Heatcock, C.H., *Introduction to Organic Chemistry*, 2nd ed., Macmillan Publishing, New York, p. 399, 1981.
(65) Ibid, p. 367.